Available online at www.sciencedirect.com
SCIENCE DIRECT
Icarus 180 (2006) 546–554
ICARUS
www.elsevier.com/locate/icarus

Space weathering of silicates simulated by nanosecond pulse UV excimer laser

R. Brunetto [a,b,*], F. Romano [a], A. Blanco [a], S. Fonti [a], M. Martino [a], V. Orofino [a], C. Verrienti [a]

[a] *Dipartimento di Fisica, Università di Lecce, via Arnesano, I-73100 Lecce, Italy*
[b] *INAF-Osservatorio Astrofisico di Catania, via S. Sofia 78, I-95123 Catania, Italy*

Received 17 June 2005; revised 26 September 2005

Available online 9 December 2005

Abstract

Laser irradiation experiments have been performed on powdered silicates (othopyroxene, clinopyroxene, and olivine) using a nanosecond pulse UV excimer laser (193 and 248 nm) to simulate the effects of space weathering induced on minor bodies of the Solar System by micrometeorite bombardment. We have used different fluences (from 0.05 to 2 J/cm^2) to weather the samples, experimenting below and above the ablation threshold. All the irradiated materials have shown reddening and darkening of their UV–vis-NIR reflectance spectra. In addition we have found that: (1) below ablation threshold, weathering effects increase with increasing number of laser pulses, and with increasing fluence, confirming that a thermal process is active; (2) above ablation threshold, weathering is much stronger and efficient than in the previous case, and is independent on the number of pulses. We show that astrophysical time-scales, i.e. times necessary to obtain similar effects on planetary objects, are of about 10^8 yr for both olivine and pyroxene in the case of ablation. The time grows up to 10^{10} yr in the case of thermal effects. We infer that micrometeorite bombardment can be rightly simulated by laser irradiation only considering congruent laser ablation.

Keywords: Spectroscopy; Experimental techniques; Radiation chemistry; Meteorites; Asteroids

1. Introduction

The effects induced by cosmic and solar wind ion irradiation, and by interplanetary dust (micrometeorites) bombardment on airless rocky surfaces are known as space weathering. These two processing mechanisms are believed to be active, with different intensity and effects, on a large distance scale, from Mercury (Killen et al., 2001) to the Kuiper Belt (Doressoundiram et al., 2002).

The effects of space weathering change progressively the solar reflectance spectra of airless bodies (in the UV–vis–NIR range), and include spectral darkening, reddening and subdued absorption bands (Hapke, 2001).

Space weathering was initially studied on lunar soils, since lunar soils returned from Apollo missions have optical properties that differ significantly from those of pristine lunar rocks (Conel and Nash, 1970). Cassidy and Hapke (1975) suggested the presence of metallic iron particle coatings on lunar soils; these coatings should be produced by deposition of atoms sputtered by solar wind particles and deposition of gaseous species produced by micrometeoritic impacts. Pieters et al. (2000) analyzed the products of space weathering of lunar soils, and demonstrated that nanophase reduced iron is produced on the surface of grains by a combination of vapor deposition and irradiation effects.

Furthermore it has been suggested that space weathering can be responsible of the significant mismatch between the spectra of the most populous class of meteorites (ordinary chondrites, OC) and the surface spectra of S-type NEOs (Near Earth Objects) and MBAs (Main Belt Asteroids), their presumed asteroidal parent bodies (Jedicke et al., 2004; Lazzarin et al., 2004). Indeed, Chapman (1996) proposed space weathering as an active process able to explain the color variations of the surface of Asteroid 243 Ida measured by the Galileo spacecraft.

The evidence that micrometeorite bombardment and solar wind ion irradiation would tend to convert spectra of ordi-

* Corresponding author. Fax: +39 0832 297505.
E-mail address: rbrunetto@ct.astro.it (R. Brunetto).

0019-1035/$ – see front matter
doi:10.1016/j.icarus.2005.10.016

nary chondrites, i.e. fresh materials, to have the spectral traits of S-type asteroids, lies on successful laboratory experiments. Laboratory simulations have been performed on asteroid-like materials simulating solar wind and cosmic ion irradiation by keV–MeV ion irradiation, and assuming that micrometeorite bombardment can be simulated by laser irradiation.

In spite of previous results (Dukes et al., 1999; Yamada et al., 1999) of ion irradiation experiments using H^+ and He^+ ions, which caused only small changes in the spectra, Strazzulla et al. (2005) performed ion irradiation of ordinary chondrite Epinal (H5) with Ar^{2+} 60 keV, producing strong darkening and reddening of the Vis–NIR spectra.

An explanation of this discrepancy is given by Brunetto and Strazzulla (2005), who have performed ion irradiation experiments of bulk silicates, using different ions having different energies (60–400 keV); they have found that the increase of the 1 μm band spectral slope is strongly related with the number of displacements caused by colliding ions inside the sample. This implies that reddening and darkening in ion irradiation experiments can be attributed to creation of displacements for fluence lower than 10^{17} ions/cm^2 (Brunetto and Strazzulla, 2005), and to sputtering of iron and deposition of nanophase neutral Fe on adjacent grains for fluence higher than 10^{18} ions/cm^2 (Hapke, 2001).

Comparing spectra of irradiated samples of Epinal with those of some S-type NEOs, Strazzulla et al. (2005) found that solar wind weathering is very efficient, and the time-scale for the reddening process is of the order of 10^5 yr at about 1 AU (Astronomical Unit) from the Sun.

Ion irradiation experiments can be considered a direct reproduction of solar wind irradiation effects; on the contrary, laser irradiation is assumed to simulate micrometeoroid impacts, but the confidence of this assumption is somewhat unclear. The most important point for a correct simulation by laser irradiation is the use of nanosecond pulses, in order to reproduce the duration of the vaporization process induced by micrometeorite impacts.

Laser irradiation effects are known to vary widely, depending on the wavelength of the incident laser beam, on the energy fluence (J/cm^2) of the single pulse, on the pulse duration, on the repetition rate, on properties of the target, etc. (Chrisey and Hubler Eds., 1994). In particular varying the laser fluence, it is possible to distinguish two main regions: at low fluence, laser irradiation induces mainly thermal and chemical effects, on the contrary ablation occurs when the laser-light intensity is high enough to induce significant material vaporization so that a dense vapor plume is formed. The threshold fluence value to achieve ablation strongly depends on the properties of the target and on the laser parameters: with inorganic insulators and strong-to-medium absorption, threshold fluence is typically between 0.5 and 2 J/cm^2 per pulse (Bauerle, 2000), valid for nanosecond pulsed laser. Indeed, the threshold value is not independent on the pulse length.

Furthermore, achieving the congruent ablation regime depends not only on experimenting above the threshold, but also on letting the laser radiation being absorbed in the very upper layers (few tens of nm) of the material, to avoid the uncontrolled heating of the surrounding target.

Actually, the first experiments to simulate space weathering of OCs (Moroz et al., 1996) were performed using microsecond pulsed laser irradiation to redden and darken reflectance spectra. Nevertheless, the laser pulse duration was much longer than the reasonable timescale of micrometeorite (1–10 μm size) impacts, and, according to Sasaki et al. (2001), the resultant spectral changes should be ascribed to glass formation.

A shorter pulse duration (6–8 ns) was consequently used in a number of experiments described by Yamada et al., 1999; Sasaki et al., 2001, and Hiroi and Sasaki, 2001. They used a nanosecond pulsed Nd-YAG laser ($\lambda = 1064$ nm) on pellets of pressed silicate powder, inducing vaporization and redeposition processes. Such experiments showed progressive (increasing the shot number) darkening and reddening of the UV–vis–NIR silicate spectra, whose comparison with asteroid spectra led to a time-scale for this process (in the near-Earth space) of about 10^8 yr. They attributed the observed spectral weathering to formation of coating enriched in vapor-deposited nanophase iron (Sasaki et al., 2001).

It is well know that the characteristics of the ablation process strongly depend on laser parameters, and target properties. The interaction between radiation and matter (as ruled by the considered regime) depends on the particular balance of optical properties, laser fluence, duration of the pulse, wavelength of the laser, etc. In particular, when an infrared Nd:YAG laser (1064 nm) is considered, like in the experiments of Yamada et al. (1999) and Sasaki et al. (2001), pulsed laser ablation can simply be treated as a thermal process: infrared laser light excites vibrations (related to defects, impurities or the solid surface itself) and the thermalization of the excitation energy is so fast that the laser can simply be considered as a heat source. With these sources at high laser light intensities ($>10^8$ W/cm^2), the interaction between the laser light and the induced plasma is dominant. The excitation energy is instantaneously transformed into heat, and the resulting increase of temperature changes the optical properties of the material, and the amount of absorbed laser power. In this regime, the irradiated material becomes absorbing at any wavelength due to surface breakdown and plasma formation. The temperature rise can result in thermal material ablation.

A typical problem with infrared lasers is a surface damage due to uncontrolled melting or ablation of the target; moreover the temperature rise induces stresses which can also affect the optical properties of the surrounding materials.

With ultraviolet laser radiation the situation can be quite different. If the photon energy is high enough, laser light excitation can result in a direct bond breaking: as a consequence, single atoms, molecule clusters, and/or fragments desorbs from the surface. Furthermore, high photon energies (i.e. short wavelength) allow spatially well defined and stoichiometric ablation (congruent ablation), rapid heating and cooling rates with low damage of the surrounding materials.

In this paper we present the results of laser irradiation experiments that we have performed on pellets of powdered silicates, having different composition (orthopyroxene, clinopyroxene,

olivine); we use a nanosecond pulse UV excimer laser, at two different wavelength, 193 and 248 nm, to simulate the effects of space weathering induced on minor bodies of the Solar System by micrometeorite bombardment.

Actually, at the present time nobody knows what is the closest simulation to space-weathering process. For instance, uncontrolled melting could be a part of the phenomenon occurring in micrometeorite impacts onto airless bodies. In this respect, our experiments are aimed to extend the previous results, by considering a larger number of experimental situations.

Indeed, different fluences, from 0.05 to 2 J/cm^2, are used to weather the samples, experimenting below and above the ablation threshold. The irradiated and ablated targets are studied by modifications of their UV–vis–NIR reflectance spectra and XPS (X-ray Photoelectron Spectroscopy) analysis.

2. Experimental setup

The experimental setup used to irradiate and ablate the samples consists of a multigas pulsed excimer laser (Lambda Physics LPX 305i), a multitarget stainless steel chamber and a pumping system.

Irradiations below the ablation threshold (hereinafter BAT irradiation) were performed with a KrF excimer laser, working at a wavelength of 248 nm with pulse duration of about 20 ns. The laser beam was homogenized by a fly's eye beam homogenizer optimized to work at 248 nm (Microlas), and directed perpendicularly to the sample. The homogenized laser spot on the sample surface was of 0.9×0.9 cm^2, while the energy per pulse of the laser beam was varied in the range 43–105 mJ, obtaining fluences in the range 0.05–0.13 J/cm^2. The number of laser pulses was changed from 1000 to 20,000.

Ablation of the samples was performed by an ArF excimer laser operating at 193 nm with pulse duration of 20 ns. In this case the laser beam was focused by a lens and then directed onto the target at an angle of 45° to have a spot of about 1.5 mm^2, so that the laser fluence was about 2 J/cm^2. The targets were mounted vertically on a holder, which can support up to three different targets. Two different type of motions (spinning and spanning) are possible for the targets, in order to irradiate a given area of the samples, and ablate it uniformly. Therefore, a certain number of pulses is needed to cover a single cycle of motion; further pulses correspond to further passages and ablation on the same area.

The duration of our laser pulse (about 20 ns), typical for an UV excimer laser, is longer than the 7 ns duration used by Yamada et al. (1999). However, only a change of orders of magnitude (regime of picoseconds, or femtoseconds, etc.) would cause strong differences in the physical process. For instance, lengthening the duration to microseconds one would get effects similar to those described in the paper by Moroz et al. (1996). So, we believe that the difference between 20 and 7 ns has little influence on the results.

The total dose (measured in J/cm^2), in case of irradiation below ablation threshold is given by: dose = fluence × number of pulses; while in case of ablation it is given by: dose = laser energy × number of pulses/ablated area. Note that, at a given fluence, a large number of pulses may correspond to the lower dose in an increased ablated area, i.e. to about a single complete cycle of motion (spinning and spanning) of the target.

In case of ablation, a silicon substrate was positioned parallel to the targets in order to collect the ablated material (film deposition); the distance from target to the substrate was 50 mm. Both BAT (below ablation threshold) irradiation and ablation were performed in a vacuum chamber, evacuated down to 5×10^{-5} Pa, with a frequency of pulses of 10 Hz.

It has to be stressed that, differently from the case of Yamada et al. (1999) and Sasaki et al. (2001) where the samples were placed horizontally, with our experimental setup the targets can be mounted only vertically; this leads to a diverse profile of the plume and a minor amount of re-deposited material. This difference has to be kept in mind when comparing the spectral modifications.

Directional-hemispherical reflectance spectra have been collected using a Perkin–Elmer Lambda 900 spectrophotometer in the UV–vis–NIR spectral range (0.25–2.5 μm), equipped with a Labsphere integrating sphere of 150 mm diameter in Spectralon. The error in the reflectance spectra was of about 5%.

The laser irradiation covered homogeneously areas of about 0.5–0.8 cm^2, while the beam spot size in the reflectance measurements was about 0.1 cm^2, so that the reflectance measurements after irradiation referred only to the irradiated area.

In addition, XPS measurements have been performed at SuperLab (Laboratory of Surfaces and Interfaces), Consorzio Catania Ricerche, University of Catania (Department of Chemical Sciences); XPS analyses were performed with an XPS spectrometer KRATOS ES 300 (180° hemispherical electrostatic analyzer) and Mg$K\alpha$ excitation (1253.6 eV) at 15 kV × 15 mA power. The pressure in the chamber was less than 10^{-7} Pa. The binding energy scale was calibrated by using several known lines.

3. Spectral modifications

We have irradiated pellets of pressed (about 8 t for 60 s) silicate powders having an average grain size of about 200 μm. Our samples are $(Mg,Fe)_2SiO_4$ olivine, $(Mg,Fe,Ca)SiO_3$ orthopyroxene and clinopyroxene, which are supposed to be the most relevant minerals for S-type asteroids (Gaffey et al., 1993). Olivine comes from San Carlos, Arizona (USA), while pyroxenes come from Bamble (Norway).

The UV–vis–NIR reflectance spectra of our samples (as prepared) are shown in Figs. 1–3, for clinopyroxene, olivine, and orthopyroxene, respectively. The spectrum of olivine before, laser treatment (labeled (1) in Fig. 2) exhibits a very strong and broad band at about 1 μm (band I); this band I is also present in pyroxene (see Figs. 1 and 3), along with a broad band (band II), characteristic of pyroxene but not olivine, whose peak position is at about 1.85 μm in the case of orthopyroxene, and at about 2.3 μm in the case of clinopyroxene. Consequently, the ratio of band II area to band I area (BII/BI area) is sensitive to the relative amount of pyroxene to olivine in the samples; peak position of band I is known to shift towards lower wavelengths moving from olivine to orthopyroxene (Gaffey et al., 1993). Minor ab-

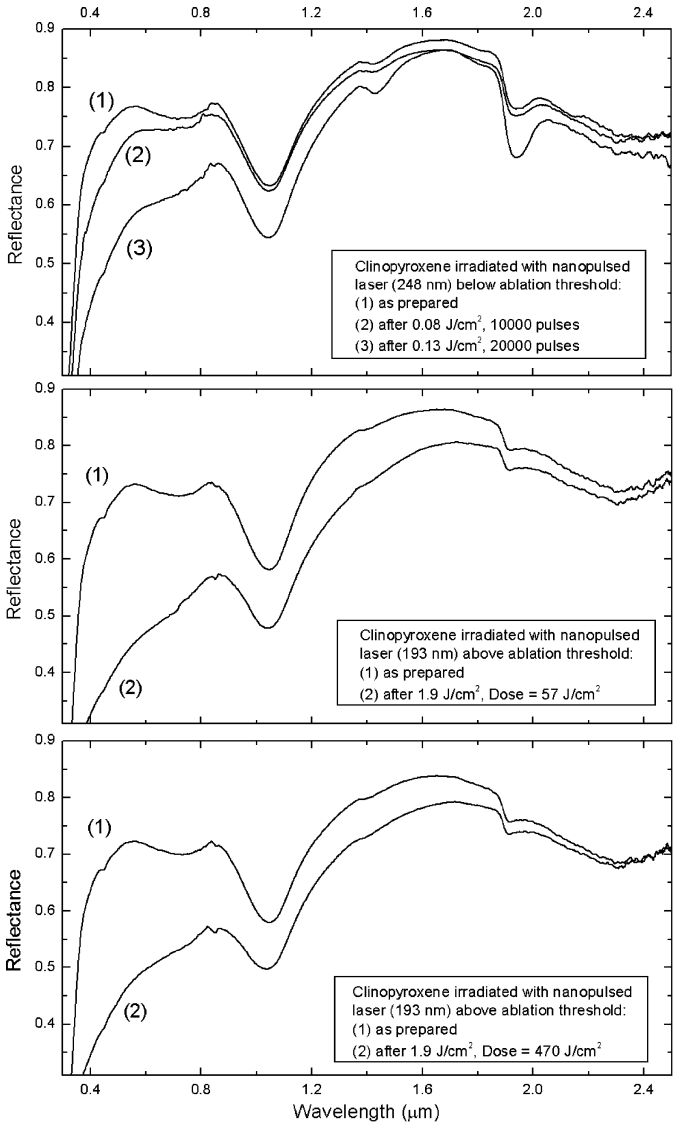

Fig. 1. Reflectance spectra of clinopyroxene samples before and after irradiation; samples have been irradiated both below (BAT, upper panel) and above (central and lower panels) ablation threshold. Darkening and reddening are stronger in the case of ablation. Spectra in the upper panel have stronger OH features, depending on the pellet preparation conditions.

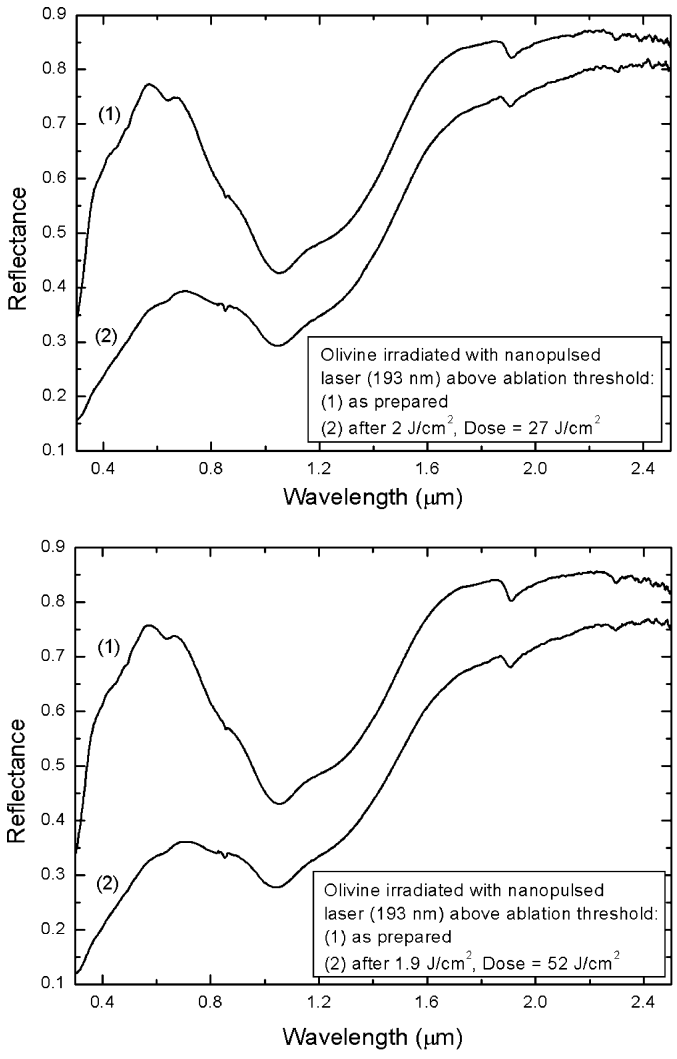

Fig. 2. Reflectance spectra of olivine samples before and after ablation; samples have been irradiated above ablation threshold, with two different doses.

sorption features are observed in the spectra at about 1.4 and 1.9 μm, due to OH absorptions that are present in the samples, and vary in intensity, depending on the pellet preparation conditions.

The clinopyroxene samples have been irradiated both below (Fig. 1, upper panel) and above (Fig. 1, central and lower panels) ablation threshold.

In the case of BAT irradiation, we have varied both the fluence of the single laser pulse, and the number of pulses. Reddening (lower reflectance at lower wavelengths) and darkening of the clinopyroxene reflectance spectra are evident; these effects increase in intensity with increasing fluence and number of pulses, i.e. with increasing dose = fluence × number of pulses.

The frequency of pulses is 10 Hz, so the time interval between pulses is 0.1 s. This is long enough (with respect to the duration of the pulse) to assure the independency of the effect of each pulse, which should avoid heat accumulation; we have also verified that varying the frequency to 1 Hz, the spectral changes are the same. Thus, in this frequency range, the reddening is independent on the frequency itself.

Also in the case of ablation, the reflectance spectra of clinopyroxene show pronounced darkening and reddening in the UV–vis–NIR range, even stronger than in the BAT irradiation case. Furthermore, in the ablated target, the weathering effects are independent on the total dose released by the laser. (Remember that in the case of ablated samples, the total dose is given by: dose = laser energy × number of pulses/ablated area.) Similar results are obtained in the case of ablated olivine (Fig. 2) and ablated orthopyroxene (Fig. 3). In all of the ablated samples, an intense plume of ejected material was observed, and deposition of those vaporized material was realized on silicon substrates resulting in the production of amorphous silicate films. Analysis of these deposits, by means of a Scanning Electron Microscope, is planned in forthcoming experiments.

We observe that in the case of olivine, a dose of 27 J/cm^2 is able to induce strong darkening and reddening; in our experi-

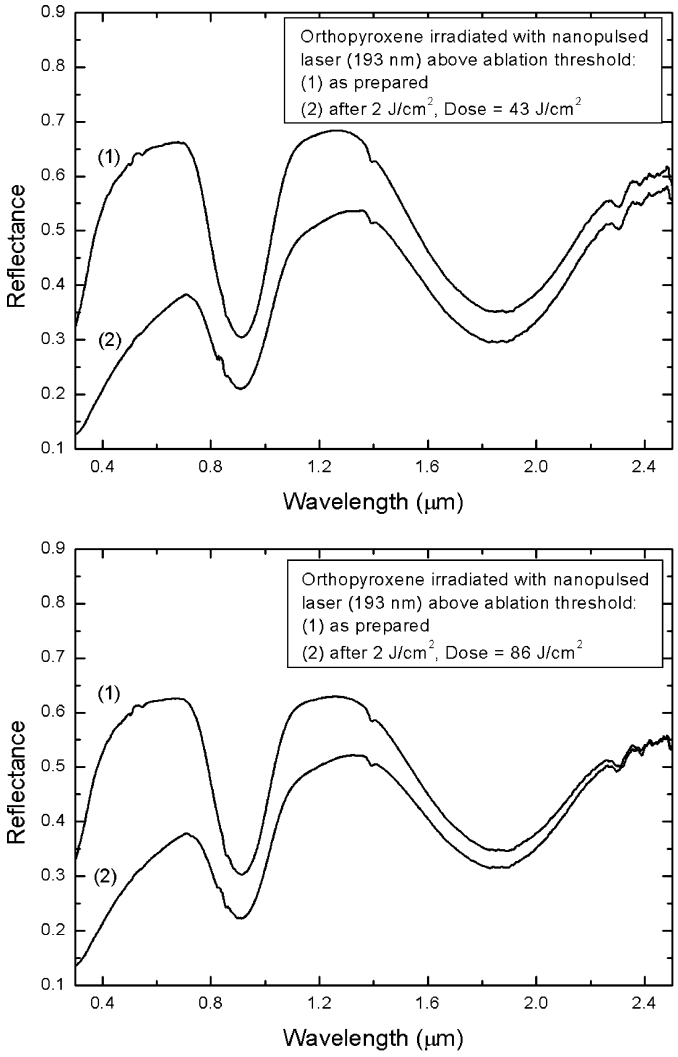

Fig. 3. Same as Fig. 2, but for orthopyroxene samples.

mental conditions, this dose value corresponds to about a single complete cycle of motion (spinning and spanning) of the target. This means that, in UV ablating conditions, a single passage of the laser on the sample surface is sufficient to induce the observed weathering effects, whose intensity does not change with further repeated ablation cycles.

In order to quantify the produced weathering effects, and to compare them with those observed in asteroids and previous laser irradiation experiments (Yamada et al., 1999), we have scaled the reflectance spectra to 1 at 0.55 μm, and have consequently evaluated the spectral slope, as the slope of a linear continuum across band I (as described by Gaffey et al., 1993, or by Hiroi and Sasaki, 2001). The scaled spectra are plotted in Fig. 4; different samples of the same end-member silicate may slightly differ in the initial spectral slope. From Fig. 4, it is apparent that ablated clinopyroxene reaches spectral slopes higher than BAT irradiated clinopyroxene, implying that weathering effects are more efficient for ablation than for BAT irradiation. Moreover, Fig. 4 shows that ablated olivine reaches the highest slope observed in this work; this is in agreement with what reported by Hiroi and Sasaki (2001), who found that olivine is weathered at higher level than pyroxene.

4. Discussion

Since the spectral slope is a good parameter to describe the weathering of silicates, we have analyzed the slope value as a function of fluence and number of pulses, for clinopyroxene. Results are plotted in Fig. 5: in the left panel the fluence is fixed, while in the right panel the number of pulses is fixed. Below the ablation threshold, the spectral slope increases linearly with both increasing fluence or number of pulses.

In the left panel of Fig. 5, we include also the points of ablated clinopyroxene. The point at about 1000 number of pulses corresponds to about two complete cycles of the motion of the target; this comparison shows that ablation is much more efficient, and that the first cycles are enough to reach the highest slope.

The difference between the two regimes has to be ascribed mainly to the different effects of the interaction of the laser with the target surface. Irradiation of a solid with a laser fluence below the ablation threshold, induces changes in the morphology and microstructure of the surface, generation of defects and depletion of one or several components of the target. Even for very low fluences, laser-induced desorption of a single or few monolayers, or the depletion of a single species take place.

On one hand (left panel of Fig. 5), increasing the number of pulses the effects of the interaction become more marked; on the other hand (right panel of Fig. 5), also increasing the laser fluence causes an increasingly spectral reddening, because the depletion of one particular material component is known to increase with fluence. It is important also to note that the laser fluence corresponding to different degrees of surface damage and depletion depends on the particular material and laser parameters.

On the contrary, let us consider the experiments with fluence higher than ablation threshold: in our conditions (high laser power densities, short pulses and short laser wavelength) the ablation mechanism takes place on a time-scale short enough to suppress the dissipation of the excitation energy beyond the volume ablated during the pulse; consequently, the segregation of the remaining target into different components can be largely avoided. In this regime of interaction, the relative concentration of species within the plasma plume remains almost unchanged for successive laser pulses and equal to those of the target, resulting in congruent ablation. In this regime heat loading of the target and material segregation remain small.

This scenario can give an explanation of the different spectral behavior; in case of ablation the highest slope is almost immediately reached. The effect is then saturated: a further increase in the number of laser pulses has only the effect of ablating material of the same composition of the starting target, i.e. the grains fly away from the pellet. The darkening and reddening of the reflectance spectra can be probably attributed to changes in the morphological structure of the sample surface after interaction, rather than formation of nanophase Fe parti-

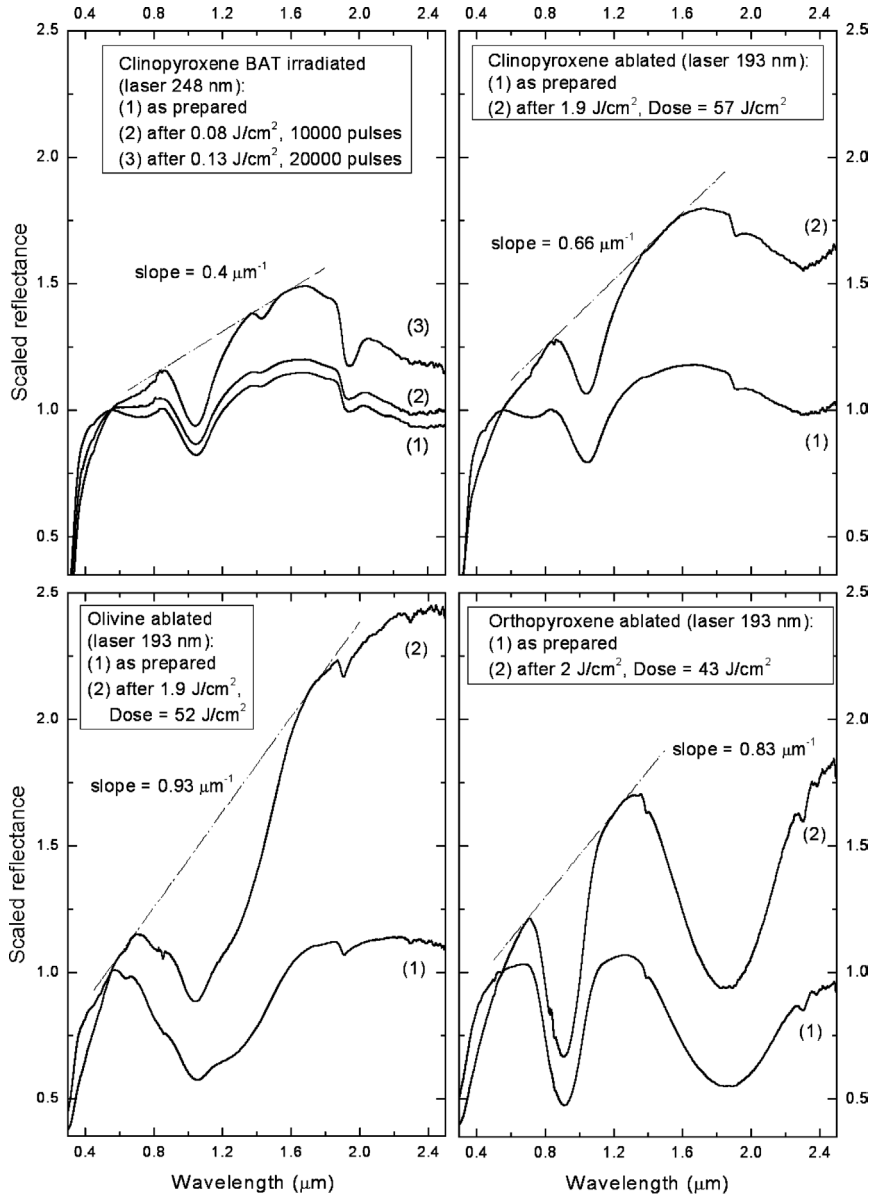

Fig. 4. Scaled reflectance spectra of clinopyroxene, orthopyroxene, and olivine, before and after irradiation, below and above ablation threshold. The values of the final spectral slopes are reported, showing that ablated olivine reaches the highest slope.

cles, as it is discussed below. However, a detailed microscopic analysis of the sample surfaces is necessary to draw meaningful conclusions and this will be performed in forthcoming studies.

The linear increase of spectral slope, shown in Fig. 5 for clinopyroxene below ablation threshold, implies that the slope value of BAT irradiated samples increases linearly with increasing laser dose. This is also shown in Fig. 6, where we plot the spectral slope vs. dose: we include the points from our samples (BAT irradiated and ablated), and the values for olivine and orthopyroxene as derived by the published data of Hiroi and Sasaki (2001); in their experiments, both laser energy and number of pulses were varied, so that it is possible to plot their spectral slopes vs. the total dose; in particular they ablated olivine and orthopyroxene using an IR laser, up to a dose of 24 and 480 J/cm^2, respectively.

Also the points from Hiroi and Sasaki (2001) follow a linear trend with increasing dose. Nevertheless, their experimental values seem to be somehow in between our results obtained in BAT irradiation and ablation regimes. Indeed, Fig. 6 reveals that there are some differences between our ablation experiments and those of Hiroi and Sasaki (2001): while they had to increase the dose to reach the highest slopes, in our ablation experiments the slope is not influenced by the dose, i.e. we observe the strongest reddening already at the first dose; furthermore, the slopes values that we obtain for both ablated olivine and ablated orthopyroxene are about 50% higher than those of Hiroi and Sasaki (2001).

The comparison between UV and IR is referred to the total dose, and scaled to the power of the laser, so that the difference between the two regimes is intrinsically connected with the dif-

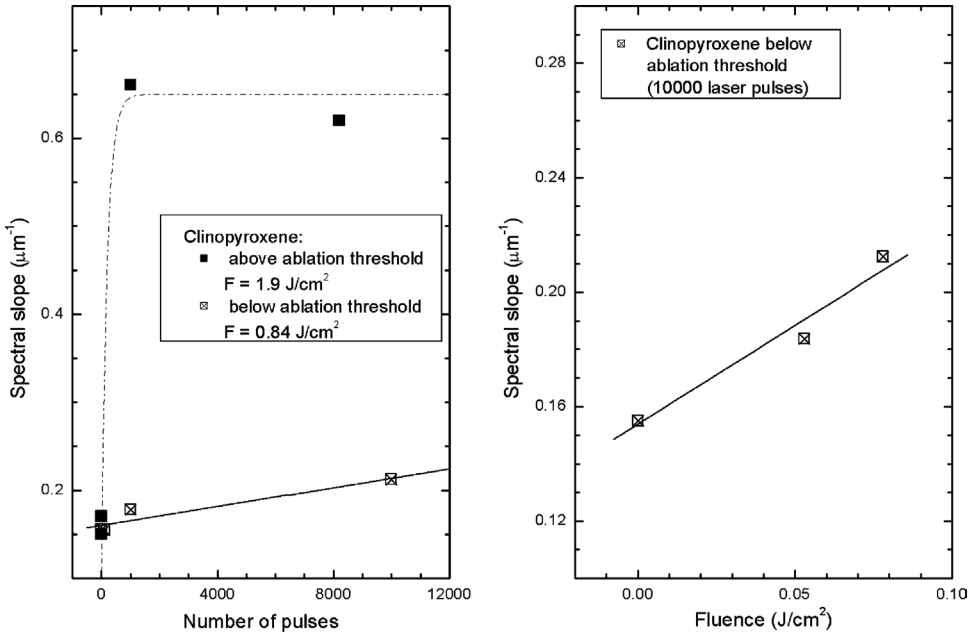

Fig. 5. Left panel: spectral slope of clinopyroxene vs the number of pulses, below and above ablation threshold. Right panel: spectral slope of clinopyroxene vs the laser fluence, in case of BAT irradiation.

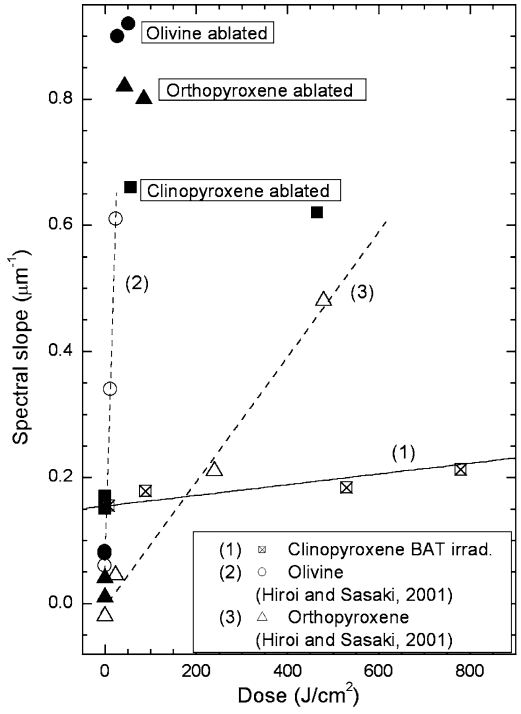

Fig. 6. Spectral slope vs the total dose, for our experiments below (crossed points) and above (full points) ablation threshold, on clinopyroxene (squares), orthopyroxene (triangles), and olivine (circles). Also the values for orthopyroxene and olivine (open triangles and circles) from Hiroi and Sasaki (2001) and Yamada et al. (1999) are included.

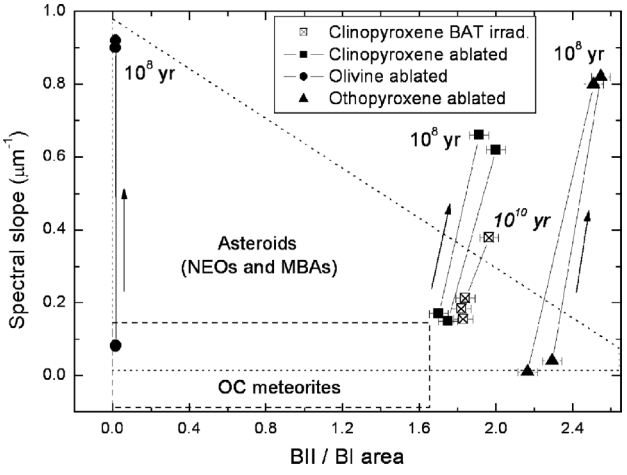

Fig. 7. Spectral slope vs the BII/BI area ratio, for our experiments below (crossed points) and above (full points) ablation threshold, on clinopyroxene (squares), orthopyroxene (triangles), and olivine (circles). The asteroid and meteorite regions are displayed, as derived by the data of Marchi et al. (2005). The arrows mark the direction towards which space weathering by micrometeorite impacts should act. The astrophysical time-scales are given, as derived in the text.

ferent mechanism: such discrepancies can be explained by the fact that we use a UV laser.

In the case of UV laser a strong absorption of laser light is guaranteed by the very short wavelength. In this case it is possible to limit thermal effects onto the target and consequently a regime of congruent ablation occurs. On the contrary, with IR laser sources it is necessary to take into account the heat loading of the target, and the consequent damage occurring in the surrounding material.

Nevertheless, since also uncontrolled melting could be a consequence of a micrometeorite impact, it is not easy to say which is the closest simulation to space weathering process. Consequently, Fig. 6 has to be seen as an extension of the previous results by Hiroi and Sasaki (2001); however, Fig. 6 clearly shows that congruent laser ablation is the most efficient condition to redden silicate spectra.

As a proof that we have been experimenting in conditions of congruent ablation, we have performed XPS analyses of

the olivine sample before and after UV laser ablation. These analyses have shown that there are no considerable variations of the chemical composition of the weathered target, whose atomic percentage values are: O, 56.6%; Si, 13.2%; and Mg, 30.2%, which lie within a 1% deviation from the measured initial composition: O, 56.9%; Si, 13.9%; and Mg, 29.2%. These values are close to those of pure forsterite (iron poor olivine); indeed in our olivine target the Fe content is undetectable by XPS measurements, i.e. it is in the order of 1–2%. This implies that spectral reddening can be observed also in iron poor silicates.

Since the iron content is on the order of 1–2%, we think that formation of nanophase Fe particles should be negligible in our case. Anyway, we cannot draw definitive conclusions, and in this respect a detailed analysis of the sample surfaces will be performed in forthcoming studies, along with magnetic analyses like those described by Bentley et al. (2005).

Moreover, we remind that, differently from the case of Yamada et al. (1999) and Sasaki et al. (2001), in our experiments the targets are mounted vertically, so that in our case a minor amount of material is redeposited. Thus, it is possible that the different configuration (vertical and horizontal) of the two experiments may have two different applications: our results could be applied to the case of smaller asteroids (lower redeposition), while those of Sasaki et al. (2001) could be the case of larger bodies (higher redeposition).

5. Astrophysical implications

The spectra of irradiated silicates should be able to explain the spectral mismatch between meteorites and asteroids. To test whether our BAT irradiation and ablation experiments can explain this space weathering effect, we have calculated the ratio of band II area to band I area (BII/BI area) as described by Gaffey et al. (1993), and then compared the spectral slope and the BII/BI area of our experiments with those of near-Earth and Main-Belt silicate rich asteroids reported by Marchi et al. (2005). In their slope vs BII/BI area plot, Marchi et al. (2005) have revealed the presence of a rectangle zone occupied by OC meteorites (defined as zero damage zone), and a triangle shaped distribution for asteroids; these two regions overlap only partially, and this is believed to be due to space weathering.

In Fig. 7 we have plotted the spectral slope vs the BII/BI area ratio of our experimental data along with the meteorite and asteroid zones. It is clear that all the slopes observed in the case of asteroids can be reproduced by our laser experiments, whatever is the composition, i.e. pyroxene to olivine ratio, of the target.

We observe that space weathering mainly acts on the slope, but that in the case of pyroxene it also causes an increase of the BII/BI area ratio; this is in agreement with what found by Ueda et al. (2002).

In order to get an astrophysical time-scale for the process, we follow Sasaki et al. (2001) who calculated a time-scale of about 10^8 yr in space at about 1 AU: they reported that, considering an impact rate of few 10^{-4} m^{-2} s^{-1} for dust particles of about 10^{-12} g (1 μm in diameter), and assuming an impact velocity of 20 $km\,s^{-1}$ for vaporization, the energy release rate by dust impacts is about 10^{-3} $J\,m^{-2}\,yr^{-1}$. The dose that we provide to redden our olivine samples is 27 $J\,cm^{-2}$: this leads to a time-scale of about 10^8 yr at 1 AU (similar results are obtained for ablated clinopyroxene and orthopyroxene); we stress that on a comparable time-scale we get higher spectral slopes than Sasaki et al. (2001), by a factor of about 50%, once again implying that UV excimer laser is more efficient than infrared laser in reddening silicate samples.

We have repeated the same calculation as before in the case of BAT clinopyroxene (irradiated below ablation threshold), finding a time-scale of about 10^{10} yr at 1 AU, i.e. longer by a factor of 100 with respect to the ablated targets.

As stated above, laser irradiation experiments simulate micrometeorite impacts whereas ion irradiation simulates solar wind irradiation. However, a direct comparison between the two cases is not easy, because the two processes are very different. In terms of energy, it is likely that the two effects have comparable efficiency in reddening silicate spectra; however, in terms of astrophysical timescale, solar wind irradiation seems to be faster (about 10^6 yr), as discussed by Brunetto and Strazzulla (2005). Nevertheless, since the ion fluxes and the micrometeoroid fluxes in space are only partially know, and they vary moving within the Solar System, the relative efficiency of the two processes may strongly change when considering different objects.

In conclusion, we have confirmed and extended the results of Sasaki et al. (2001); we have found that, in order to simulate micrometeorite bombardment, the most efficient experimental conditions to darken and redden the reflectance spectra are obtained performing congruent laser ablation, i.e. to use an UV laser with fluence higher than ablation threshold. We have found that in these conditions, spectral modifications are not caused by chemical effects, as validated by XPS analysis of the altered surface, and should rather be ascribed to alteration of the structure and morphology of the target surface after laser ablation.

Furthermore, it seems that congruent ablation reproduces quite well the micrometeorite bombardment, because it minimizes the thermal effects, causes a high transfer of momentum, and reproduces the astrophysical weathering in reasonable time-scales (10^8 yr at 1 AU). On the contrary, irradiation below ablation threshold, even if inducing similar spectral modifications, would correspond to astrophysical time-scales longer than the age of the Solar System.

However, it is possible that, in a micrometeorite impact, uncontrolled melting can occur; the amount of this melting will vary depending on the parameters of the impact (energy, velocity, angle, etc.): varying the laser fluence, we have investigated all the possible variations of these thermal effects, demonstrating that the strongest reddening is obtained when thermal effects are minimized.

Further studies are planned to investigate microscopically the surface details and modifications which cause the strong spectral darkening and reddening of our ablated samples.

Acknowledgments

The authors are grateful to G. Compagnini and G. Strazzulla for help in the XPS analysis and for other useful suggestions. The authors thank Takahiro Hiroi and an anonymous reviewer for their helpful comments. This research was supported by the Italian Ministero dell'Istruzione, Università e Ricerca (MIUR).

References

Bauerle, D., 2000. Laser Processing and Chemistry, third ed. Springer-Verlag, Berlin.

Bentley, M.S., Ball, A.J., Dyar, M.D., Pieters, C.M., Wright, I.P., Zarnecki, J.C., 2005. Space weathering: Laboratory analyses and in-situ instrumentation. Lunar Planet. Sci. XXXVI. Abstract 2255.

Brunetto, R., Strazzulla, G., 2005. Elastic collisions in ion irradiation experiments: A mechanism for space weathering of silicates. Icarus 179, 265–273.

Cassidy, W., Hapke, B., 1975. Effects of darkening processes on surfaces of airless bodies. Icarus 25, 371–383.

Chapman, C.R., 1996. S-type asteroids, ordinary chondrites, and space weathering: The evidence from Galileo's fly-by of Gaspra and Ida. Meteorit. Planet. Sci. 31, 699–725.

Chrisey, D.B., Hubler, C.K. (Eds.), 1994. Pulsed Laser Deposition of Thin Films. Wiley, New York.

Conel, J.E., Nash, D.B., 1970. Spectral reflectance and albedo of Apollo 11 lunar samples: Effects of irradiation and vitrification and comparison with telescopic observations. Apollo 11 Lunar Sci. Conf. 3, 2013–2023.

Doressoundiram, A., Peixinho, N., de Bergh, C., Fornasier, S., Thébault, P., Barucci, M.A., Veillet, C., 2002. The color distribution in the Edgeworth–Kuiper Belt. Astron. J. 124, 2279–2296.

Dukes, C.A., Baragiola, R.A., McFadden, L.A., 1999. Surface modification of olivine by H^+ and He^+ bombardment. J. Geophys. Res. 104, 1865–1872.

Gaffey, M.J., Burbine, T.H., Piatek, J.L., Reed, K.L., Chaky, D.A., Bell, J.F., Brown, R.H., 1993. Mineralogical variations within the S-type asteroid class. Icarus 106, 573–602.

Hapke, B., 2001. Space weathering from Mercury to the asteroid belt. J. Geophys. Res. 106 (E5), 10039–10073.

Hiroi, T., Sasaki, S., 2001. Importance of space weathering simulation products in compositional modeling of asteroids: 349 Dembowska and 446 Aeternitas as examples. Meteorit. Planet. Sci. 36, 1587–1596.

Jedicke, R., Nesvorný, D., Whiteley, R., Ivezic, Z., Juric, M., 2004. An age–color relationship for Main-Belt S-complex asteroids. Nature 429, 275–277.

Killen, R.M., Potter, A.E., Reiff, P., Sarantos, M., Jackson, B.V., Hick, P., Giles, B., 2001. Evidence for space weather at Mercury. J. Geophys. Res. 106 (E9), 20509–20526.

Lazzarin, M., Marchi, S., Barucci, M.A., Di Martino, M., Barbieri, C., 2004. Visible and near-infrared spectroscopic investigation of near-Earth objects at ESO: First results. Icarus 169, 373–384.

Marchi, S., Brunetto, R., Magrin, S., Lazzarin, M., Gandolfi, D., 2005. Space weathering of near-Earth and Main-Belt silicate-rich asteroids: Observations and ion irradiation experiments. Astron. Astrophys. 443, 769–775.

Moroz, L.V., Fisenko, A.V., Semjonova, L.F., Pieters, C.M., Korotaeva, N.N., 1996. Optical effects of regolith processes on S-asteroids as simulated by laser shots on ordinary chondrite and other mafic materials. Icarus 122, 366–382.

Pieters, C.M., Taylor, L.A., Noble, S.K., Keller, L.P., Hapke, B., Morris, R.V., Allen, C.C., McKay, D.S., Wentworth, S., 2000. Space weathering on airless bodies: Resolving a mystery with lunar samples. Meteorit. Planet. Sci. 35, 1101–1107.

Sasaki, S., Nakamura, K., Hamabe, Y., Kurahashi, E., Hiroi, T., 2001. Production of iron nanoparticles by laser irradiation in a simulation of lunar-like space weathering. Nature 410, 555–557.

Strazzulla, G., Dotto, E., Binzel, R., Brunetto, R., Barucci, M.A., Blanco, A., Orofino, V., 2005. Spectral alteration of the meteorite Epinal (H5) induced by heavy ion irradiation: A simulation of space weathering effects on near-Earth asteroids. Icarus 174, 31–35.

Ueda, Y., Hiroi, T., Pieters, C.M., Miyamoto, M., 2002. Changes of Band I center and Band II/Band I area ratio in reflectance spectra of olivine–pyroxene mixtures due to the space weathering and grain size effects. Lunar Planet. Sci. XXXIII. Abstract 2023.

Yamada, M., Sasaki, S., Nagahara, H., Fujiwara, A., Hasegawa, S., Yano, H., Hiroi, T., Ohashi, H., Otake, H., 1999. Simulation of space weathering of planet-forming materials: Nanosecond pulse laser irradiation and proton implantation on olivine and pyroxene samples. Earth Planets Space 51, 1255–1265.